Postprint of: Racewicz S., Riu D. M., Retière N. M., Chrzan P. J., Half-Order Modeling of Saturated Synchronous Machine, IEEE Transactions on Industrial Electronics, Vol. 61, Iss. 10 (2014), pp. 5241-5248, DOI: 10.1109/TIE.2014.2301741

Half-Order Modelling of Saturated Synchronous Machine

S. Racewicz, D. M. Riu, N. M. Retière, and P. J. Chrzan, *Member, IEEE*

***Abstract*—Noninteger order systems are used to model diffusion in conductive parts of electrical machines as they lead to more compact and knowledge models but also to improve their precision. In this paper a linear half-order impedance model of a ferromagnetic sheet deduced from the diffusion of magnetic field is briefly introduced. Then, from physical considerations and finite elements simulation, the nonlinear half-order impedance model of a ferromagnetic sheet is proposed taking into account of both saturation and diffusion effects. Next, it has been proved, that this model can be successfully included in the equivalent circuits of a synchronous machine (SM) taking into account of eddy-currents in massive parts of the rotor or damper bars and of small signal saturation. The new SM equivalent circuit is validated by stand still frequency response tests performed on the solid salient pole SM of 125 kVA for variable field excitation conditions. An example of the SM transfer function computation in relation to different magnetization levels indicates usefulness of this modelling approach for robust control issues.**

***Index Terms*—Noninteger order modelling, parameter identification, small signal saturation, SSFR test, synchronous machine equivalent circuit**

I. Introduction

Current development of embedded generation requires coming back over the modelling of supply groups in order to assess the impact of their integration on the dynamic behaviour of power systems. More precisely, it becomes necessary to improve modelling of motor and generator units in order to robustify their control as they are highly subjected to manifold disruptions or state uncertainties (load steps, saturations, faulty-conditions, etc.) [1, 2].

In this article, we have focused on synchronous machine modelling for robust control purpose [3]. It is then necessary not only to provide accurate model of machine over a wide range of frequencies, but also to identify model parameters for control synthesis. Moreover, order of the machine model has to be reduced as robust control techniques lead to high-order controllers [4]. Therefore, the system order reduction is particularly necessary to obtain reduced order controllers for an implementation feasibility.

In most generators, as frequency increases, induced currents can no longer be neglected. Equivalent circuits of synchronous machines are then improved by including ladder elements with constant parameters [5, 6, 7]. However, as diffusion effect is a distributed phenomenon described by partial differential equations, classical improved equivalent circuits must include in theory an infinite number of lumped and constant parameters. Practically, the number of parameters is chosen to meet the desired accuracy over a given frequency range [8].

In previous works, the authors have proposed an alternative way of modelling based on noninteger order systems. These systems have then been used to model diffusion in conductive parts of electrical machines. They lead to more compact and physical models but also improve their precision [9, 10]. Nevertheless, noninteger order models have been established for linear cases. It is then interesting to investigate the influence of saturation on model topology and parameter values. Indeed, for accurate analysis of generator stability performance, small signal magnetic saturation effects have to be taken into account [11]. Corresponding B-H paths in the rotor iron are then described by the incremental permeability [12], giving rise to dynamic inductances, that can be obtained from the standstill frequency response tests (SSFR) [22].

Modelling of magnetic saturation effects in wound field synchronous machine (SM), has attracted over the years much attention. In the scope of recent significant works, in [13] saturation conditions are included in the magnetizing branch, while rotor equivalent circuit is replaced by linear network. In order to reduce the complexity of finite element method, the magnetic equivalent circuit for the SM is developed in [14]. Cross-magnetization impact of two-axis frame saturated SM model as analyzed in [15], has been previously studied by anisotropic saturated SM models [16].

In this paper with the aim of SM modelling order reduction, firstly a linear half-order impedance model of a ferromagnetic sheet deduced from the diffusion of the magnetic field is briefly introduced as this model has been already detailed in previous works [9]. Then, from physical considerations, a nonlinear half-order impedance model of the sheet is proposed taking into account of both saturation and diffusion. Next, it has been proved, that this model can be successfully included in the equivalent circuits of a SM taking into account of eddy-currents in massive parts of the rotor or damper bars and of small signal saturation. The proposed model is validated by performing 3D finite elements simulations and compared with tests performed on a synchronous machine of 3 kVA working in saturated conditions. Finally Bode diagrams for different magnetization levels are analytically represented to indicate usefulness of proposed methodology to robust control design of synchronous generators and motors.

II. Half-Order Modelling of Synchronous Machine Parts

We suppose that the radius of a machine's rotor is sufficiently big for being represented as a ferromagnetic sheet of length *L*, width *l* and height *e* (Fig. 1).

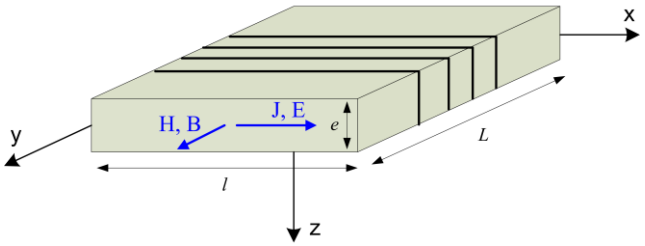

Fig. 1 Studied ferromagnetic sheet

This sheet is characterized by a permeability μ, a resistivity ρ and is surrounded by a n-turns field winding. From the diffusion equation of the magnetic field H and boundary conditions, a classical analytical model of its impedance can be expressed by (1) [17]:

$$\bar{Z}_{\text{analy}}(\omega) = j\omega \cdot L_0 \cdot \frac{\tanh(\bar{\alpha})}{\bar{\alpha}} \tag{1}$$

where L_0 is the dc inductance of the sheet, which can be expressed as:

$$L_0 = \frac{\mu \cdot n^2 \cdot e \cdot l}{L} \tag{2}$$

and:

$$\bar{\alpha}^2 = j\omega \cdot \frac{1}{\rho} \cdot \mu \cdot \left(\frac{e}{2}\right)^2 \tag{3}$$

An integer order approximation of this impedance can then be expressed from series decomposition of hyperbolic tangent function which leads to an integer order electrical circuit composed with an infinite number of RL cells [17]. Actually, this number of parameters is chosen high but finite; in this way, this model is kept accurate even if parameters may lose their physical meanings [5].

For reaching both accuracy and physical meanings, another approximation based on noninteger order systems is proposed. Thereby, the second order limited development of hyperbolic tangent function is given by (4) and (5) [9]:

$$\tanh(x) = \frac{\sinh(x)}{\cosh(x)} = \frac{\frac{e^x - e^{-x}}{2}}{\frac{e^x + e^{-x}}{2}} \underset{x\to 0}{\approx} \frac{x}{1 + \frac{x^2}{2}} \underset{x\to 0}{\approx} \frac{x}{\sqrt{1+x^2}} \tag{4}$$

$$\tanh(x) = \frac{\sinh(x)}{\cosh(x)} = \frac{\frac{e^x - e^{-x}}{2}}{\frac{e^x + e^{-x}}{2}} \underset{x\to \infty}{\approx} \frac{\frac{e^x}{2}}{e^{\frac{x}{2}}} \underset{x\to \infty}{\approx} \frac{x}{\sqrt{1+x^2}} \tag{5}$$

A half-order approximation of the analytical impedance is then given by [18]:

$$\bar{Z}^{1/2}_{\text{sheet}}(\omega) = \frac{L_0 \cdot j\omega}{\sqrt{1 + j \cdot \frac{\omega}{\omega_0}}} \tag{6}$$

with:

$$\omega_0 = \frac{1}{\frac{1}{\rho} \cdot \mu \cdot \left(\frac{e}{2}\right)^2} \tag{7}$$

The parameter ω_0 represents the cut-off frequency of the ferromagnetic sheet.

The essential point is that the infinite scaling circuit is replaced by a half-order impedance, which increases considerably the compactness of the model. Fig. 2 presents a comparison between the analytical expression (1) and its approximation using half-order system (6). The half-order model is then a good approximation of the analytical result along a wide frequency range, even if a small gap around the cut-off frequency can be noticed.

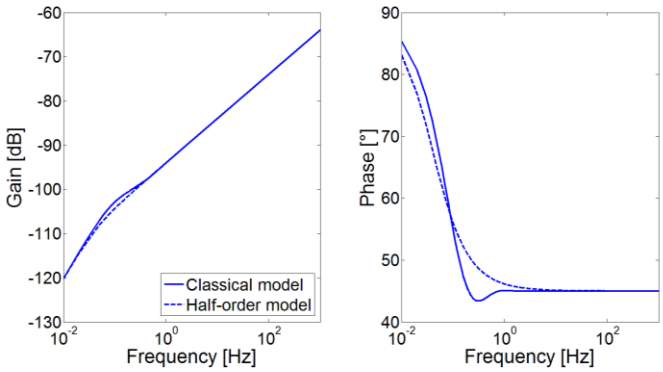

Fig. 2 Classical and half-order models of the sheet impedance

The same approach is used for rectangular copper bars modelling as shown in [9]. Then, impedance of damper bars of synchronous machine can be expressed as:

$$\bar{Z}^{1/2}_{\text{bar}}(\omega) = R_0 \cdot \sqrt{1 + j \cdot \frac{\omega}{\omega_0}} \tag{8}$$

where R_0 and ω_0 are the dc resistance and the cut-off frequency of the bar respectively.

III. Small Signal Saturation Impact

This section presents modelling of saturation appearing in a ferromagnetic sheet for small variations of the magnetic state around steady-state conditions as these models are developed for small-signal dynamic analysis and control of synchronous machine.

In general approximation, saturation of magnetic circuit is mainly apparent on the way of the mutual magnetic field lines linking stator and rotor via air gap. As only iron parts of this

way are influenced by saturation, a new model of the impedance taking into account nonlinear conditions is proposed. The frequency structure of the model presented in equation (6) is kept identical, but the dc inductance L_0 and the cut-off frequency ω_0 vary with the current:

$$\bar{Z}^{1/2}_{\text{sheet\_satur}}(\omega,i)=\frac{L_0(i)\cdot j\omega}{\sqrt{1+j\cdot\dfrac{\omega}{\omega_0(i)}}} \tag{9}$$

The evolution of L_0 and ω_0 with the current should be physically significant with a decrease of L_0 and an increase of ω_0 with current growth as relative permeability μ decreases with saturation.

In order to validate the proposed model, finite elements simulations of the ferromagnetic sheet have been done using *Flux*© software. Fig. 3 shows the modelled ferromagnetic sheet and its magnetization curve. In order to modify the magnetic saturation level, the current flowing through the winding varies from 0.01 to 20 A, which corresponds to a magnetic field strength between 0.05 and 100 A/m. For each current value impedance of the sheet is calculated with small-signal variations from 0.01 Hz to 1000 Hz. Simulation results are shown in Fig. 4. The resulting impedances are then compared to nonlinear half order impedance model (9).

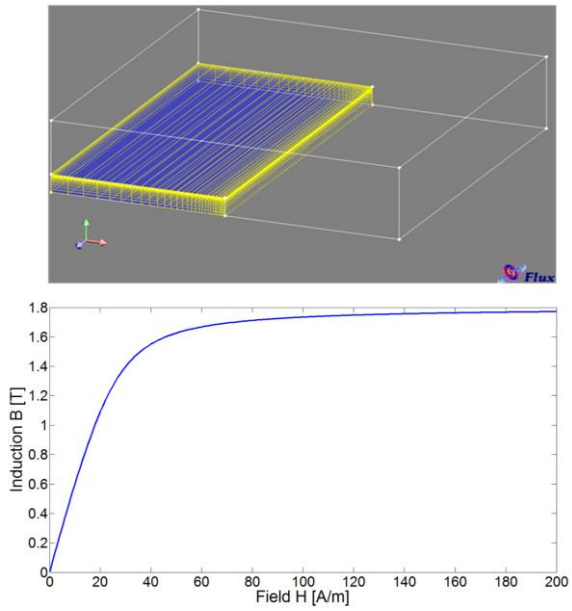

Fig. 3 Modelled ferromagnetic sheet and its saturation curve

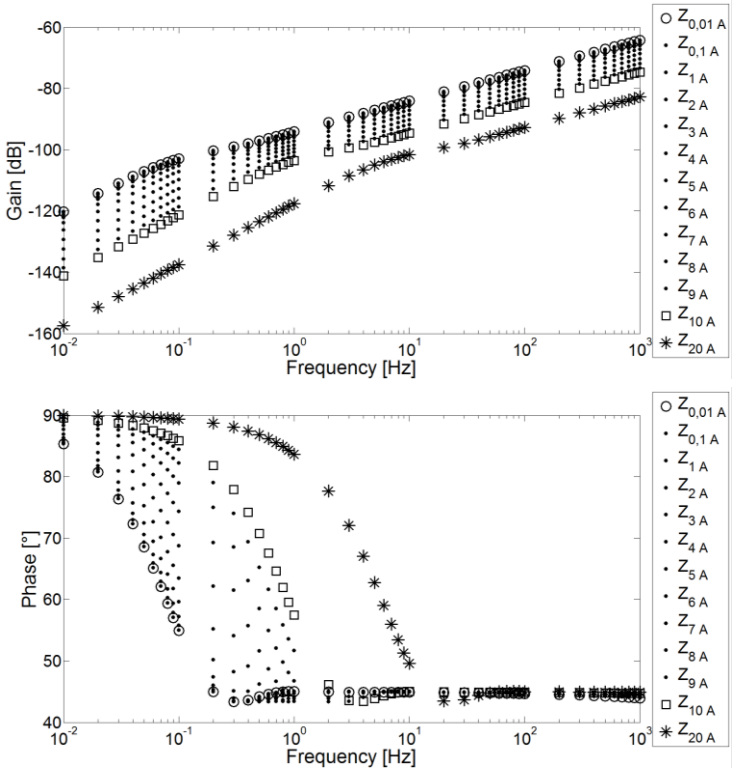

Fig. 4 Impedance of the ferromagnetic sheet for different saturation levels (from 10 mA to 20 A)

To fit the half order model and the simulation results for a given field current i, values of parameters L_0 and ω_0 are calculated analyzing the asymptotic behaviour of the half-order impedance model (9) for low and high frequencies. Finally, Fig. 5 shows the evolution of these parameters versus field current. Evolution of the parameters L_0 and ω_0 vs. the current can be approximated by mathematical equations which facilitates implementation of the model [19].

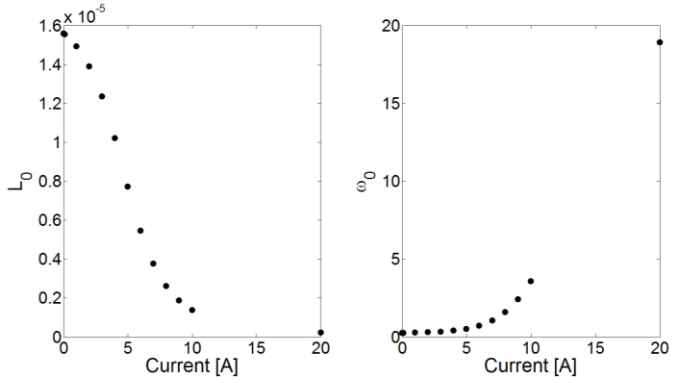

Fig. 5 Parameters L_0 and ω_0 calculated from finite element simulation results

Finally, it can be noticed, that the nonlinear half-order impedance model (9) is in very good agreement with simulations along a wide range of frequencies, as shown in Fig. 6. This model has been also validated by performing the impedance measurements on the real ferromagnetic saturated sheet [20]. This tends to prove that it could be used for modelling of synchronous generators operating in saturated conditions.

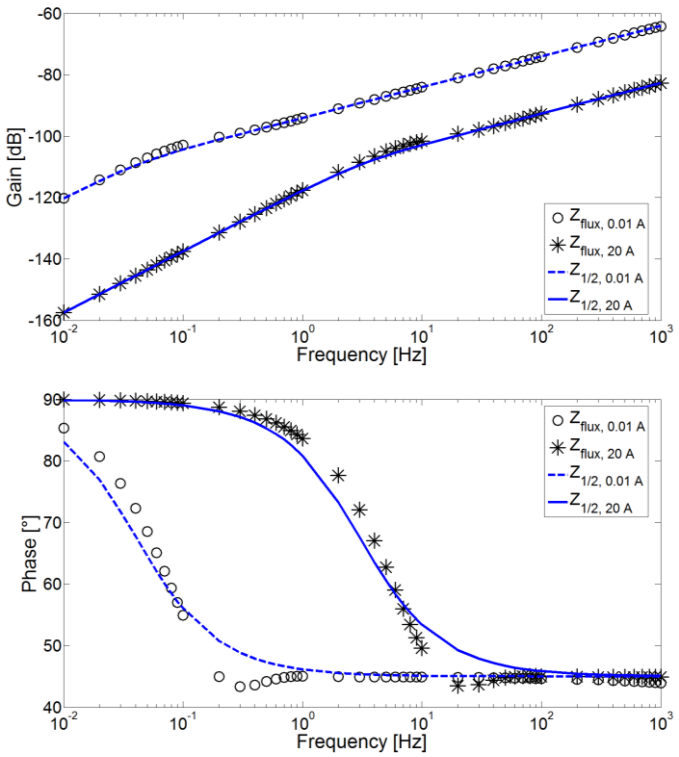

Fig. 6 Comparison of the half-order model with the finite element simulations

IV. Equivalent Circuit of Synchronous Machine

In order to model both: effects of magnetic field diffusion in conductive parts of the machine (eddy-currents) and small signal saturation of magnetic circuits, modifications of the Park equivalent circuit of synchronous generator have been proposed (Fig. 7).

Hence, in *d*-axis, stator windings are modelled by constant parameters (r_s and $l_{\sigma s}$) which are not influenced by induced currents. The differential leakage inductance (l_{f12d}) [6] is associated to the unequal magnetic coupling between stator and rotor windings and rotor windings themselves [13]. Field circuit is represented by constant parameters (r_f and $l_{\sigma f}$). Magnetic energy associated with the magnetizing current is stored in the air gap and in the rotor and stator core. The major and constant part of this energy, stored in the air gap, is represented by a constant inductance (l_{ad}). Eddy-currents in massive parts of the rotor and the rest of the magnetic energy are modelled by half-order *inductive* impedance (9):

$$\bar{Z}_{1d}^{1/2}(\omega,i)=\frac{L_{1d}(i)\cdot j\omega}{\sqrt{1+j\cdot\dfrac{\omega}{\omega_{1d}(i)}}} \tag{10}$$

Skin effects in solid conductors of damper windings are modelled by *resistive* impedance (8):

$$\bar{Z}_{2d}^{1/2}(\omega)=R_{2d}\cdot\sqrt{1+j\cdot\frac{\omega}{\omega_{2d}}} \tag{11}$$

Identical considerations are made for *q*-axis equivalent circuit construction, but there are no field parameters which results in simplifying the model. Indeed, the parameter ω_{2q} cannot be properly identified since without the field winding there is not enough information in the *q*-axis. The impedance Z_{2q} is short-circuited for high frequencies by the impedance Z_{1q}. Therefore, the damper branch in the *q*-axis described by Z_{2q} has been replaced by a resistance r_{2q} and an inductance l_{2q} constant with frequency.

Moreover, it is assumed that saturation effects in the quadrature *q*-axis can be neglected assuming significantly larger air gap of the rotor saliency. Finally, in *q*-axis equivalent circuit eddy-currents in massive parts of the rotor are modelled by half-order *inductive* impedance (6):

$$\bar{Z}_{1q}^{1/2}(\omega)=\frac{L_{1q}\cdot j\omega}{\sqrt{1+j\cdot\dfrac{\omega}{\omega_{1q}}}} \tag{12}$$

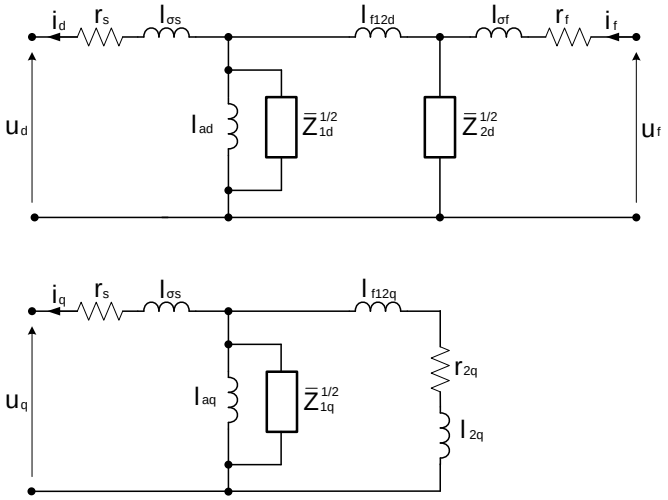

Fig. 7 Non integer order *d* and *q*-axis equivalent circuits of an alternator at standstill conditions

Parameters are then deduced from *StandStill Frequency Response tests* (SSFR) [21], and are physically representative [18]. Finally, half-order systems lead to accurate representation of dynamic behaviours over a wide range of frequencies, with a significant reduction of order.

V. SSFR Tests

A. Measurement setup

StandStill Frequency Response test (SSFR) is typically used to obtain frequency characteristics of the machine in linear conditions [21]. In comparison with other test procedures it does not require sophisticated equipment and it is harmless to the tested machine. To identify equivalent circuits with saturated half-order systems, one can use one of the method described in [22, 23, 24]. In this paper authors propose a similar method which consists on performing a regular SSFR test with a field winding fed by a controlled dc voltage source (Fig. 8).

This modified SSFR test is easy to perform and allows precise control of the machine flux.

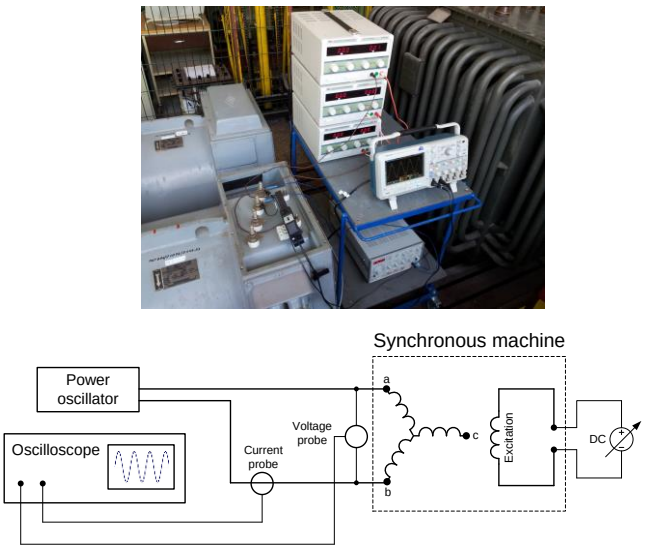

Fig. 8 Measurement setup for *d*-axis SSFR test of saturated synchronous machine

However, this configuration has a few disadvantages. First of all it allows obtaining only two operational transfer functions in *d* and *q* axis (Z_d and Z_q) defined as the ratio between armature voltage and current (V_{arm} and I_{arm}) for two rotor positions. Other transfer functions (sG and Z_{afo}), which could contribute to an accuracy of parameters estimation, require measurements of field voltage and field current, which is impossible due to the connected dc voltage source.

B. Measurements

The tests have been performed on the 125 kVA, 4-poles synchronous machine of salient rotor construction, equipped with a damper winding. Field current of the machine has been changed by steps of 2 A from 0 to 16 A (machine's nominal field current was equal to 17.4 A). For each magnetization level, series of SSFR measurements have been performed for a 0.01 Hz – 200 Hz frequency range.

Because of the high magnetization dc currents injection, even if the external cooling system has been applied, stator resistance varies slightly from 0.0261 Ω to 0.0267 Ω. In order to eliminate its influence on the operational inductance L_d (13), resistance r_s has been corrected for each magnetization level.

$$\bar{L}_d = \frac{\bar{Z}_d - r_s}{j\omega} \tag{13}$$

Results of measurements for operational inductance in *d*-axis are shown in Fig. 9. The inductance corresponding to zero field current is represented by thick solid line. Saturation effects in the quadrature *q*-axis have not been considered as in salient pole synchronous machines with electromagnetic excitation L_{aq} is practically not affected by the magnetic saturation [25].

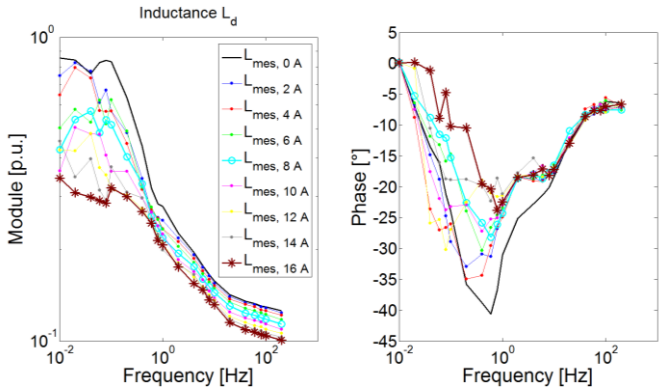

Fig. 9 Operational inductance of the 125 kVA synchronous machine for different magnetization levels (*d* axis)

C. Parameter identification

We consider then, that only parameters L_{1d} and ω_{1d} (10) are strongly influenced by saturation, especially in low frequency range.

By analyzing an asymptotic behaviour of the machine's model (Fig. 7) for high frequencies, one can find that there are three inductances which are also supposed to be influenced by saturation. These are two leakage inductances ($l_{\sigma s}$, $l_{\sigma f}$) and the differential leakage inductance (l_{f12d}). It can be noticed that each parameter $l_{\sigma s}$, $l_{\sigma f}$ and l_{f12d} has some influence on high frequency model's response. However, SSFR measurements, performed on the machine with field winding excited, do not provide sufficient knowledge allowing to identify correctly all parameters influenced by saturation. Therefore, sensitivity analysis has been performed showing in Fig. 10 the model output error variations as function of each inductance variation from -100% to +100% of pu value. Model output error is an average percentage error between measurement and model of the operational inductance L_d module for unsaturated conditions (i_f = 0 A). The above analysis has been done for the high frequency range, i.e. 20 Hz – 200 Hz. Obtained results confirmed, that the $l_{\sigma s}$ stator leakage inductance has the most pronounced effect on the model output. Hence, it has been included to model saturated machine behaviour in high frequency range.

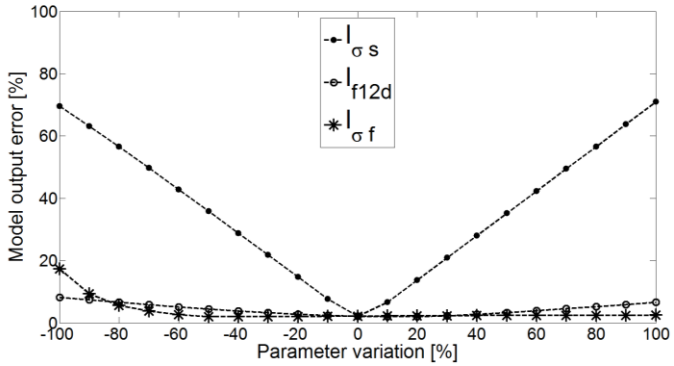

Fig. 10 Model sensitivity to the inductances variation

Identification has been done using *Matlab*® software, with the help of procedures based on least-squares and Levenberg-Marquardt optimization algorithm. After a global identification, a first set of 9 parameters has been obtained (see Table 1) for

unsaturated conditions. All of the parameters were identified at the same time using the whole frequency range. The dc voltage source was set to 0 V.

TABLE I
IDENTIFIED PARAMETERS FOR UNSATURATED CONDITIONS (I_F = 0 A)

Parameter	Value [p.u.]
r_s	0.0261
$\boldsymbol{l_{\sigma s}}$	0.0962
l_{ad}	1.0271
$\boldsymbol{L_{1d}}$	2.6960
$\boldsymbol{\omega_{1d}}$	0.0126
l_{f12d}	0.0147
R_{2d}	0.0095
ω_{2d}	0.0432
$l_{\sigma f}$	0.2202
r_f	0.0067

While the other parameters values are kept constant, parameter L_{1d} is reidentified from low frequency range only (0.01 Hz – 0.1 Hz) and for each magnetization level. The same approach is used to correct identification of $l_{\sigma s}$, but for high frequency range only (20 Hz – 200 Hz). Finally, the cut-off frequency ω_{1d} is found for each magnetization level using the whole range of frequency, taking into consideration estimated values of the parameters L_{1d} and $l_{\sigma s}$ (Table 2).

TABLE II
RESULTS OF PARAMETER IDENTIFICATION FOR DIFFERENT MAGNETIZATION LEVELS

[p.u.]	0 A	2 A	4 A	6 A	8 A	10 A	12 A	14 A	16 A
r_s	0.0261	fix	fix	fix	fix	fix	fix	fix	fix
$\boldsymbol{l_{\sigma s}}$	0.0962	0.0947	0.0923	0.0887	0.0844	0.0797	0.0756	0.0724	0.0697
l_{ad}	1.0271	fix	fix	fix	fix	fix	fix	fix	fix
$\boldsymbol{L_{1d}}$	2.6960	1.9321	1.2163	0.8767	0.6994	0.5054	0.4126	0.3643	0.2771
$\boldsymbol{\omega_{1d}}$	0.0126	0.0037	0.0087	0.0236	0.0233	0.2822	0.6024	1.3632	3.6822
l_{f12d}	0.0147	fix	fix	fix	fix	fix	fix	fix	fix
R_{2d}	0.0095	fix	fix	fix	fix	fix	fix	fix	fix
ω_{2d}	0.0432	fix	fix	fix	fix	fix	fix	fix	fix
$l_{\sigma f}$	0.2202	fix	fix	fix	fix	fix	fix	fix	fix
r_f	0.0067	fix	fix	fix	fix	fix	fix	fix	fix

As expected, the evolution of the parameters L_{1d}, $l_{\sigma s}$, and ω_{1d} (Fig. 11) is similar to the evolution from Fig. 5 for a simple saturated ferromagnetic sheet.

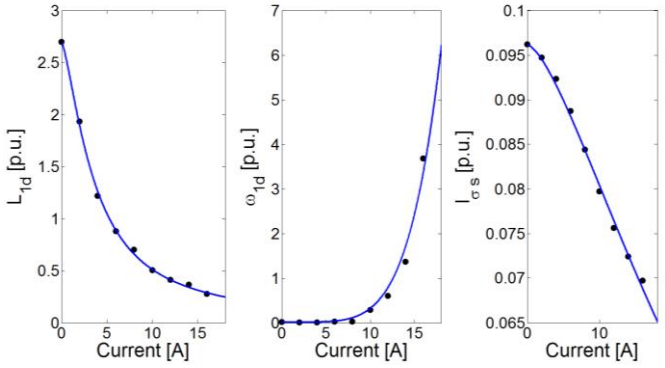

Fig. 11 Parameters L_{1d}, l_d, and ω_{1d} identification from SSFR measurements of saturated synchronous machine

It can be noticed that the model remains valid for all magnetization levels and frequency ranges (Fig. 12). Errors appearing in the phase curves are mainly linked to the fact that the parameter identification has been effectuated using only operational inductance modules. Some error is also caused by the high magnetization current injection which warms the machine being in standstill condition.

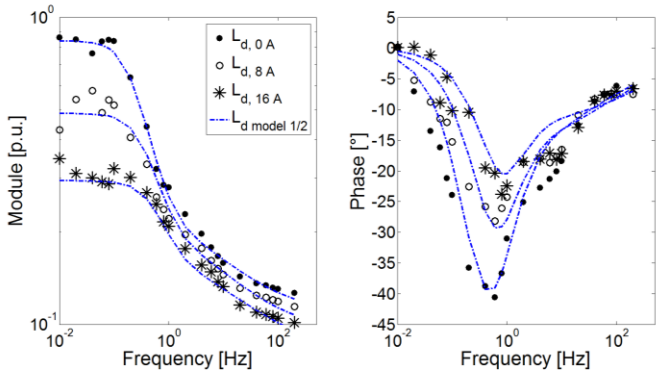

Fig. 12 Comparison of the operational inductance L_d for half-order model (dashed lines) and the SSFR measurements at different operation conditions including saturation

VI. TRANSFER FUNCTION ANALYSIS FOR ROBUST CONTROL DESIGN

Robust control of synchronous machine has to be resilient to different operating conditions variation like temperature, frequency or load changes. The load variation results in magnetic saturation level change which has a significant impact on the model parameters [22, 24].

In this section, an analysis of synchronous machine transfer function in relation to magnetic saturation levels is presented.

Fig. 13 presents block diagram of the classical small signal control of synchronous generator.

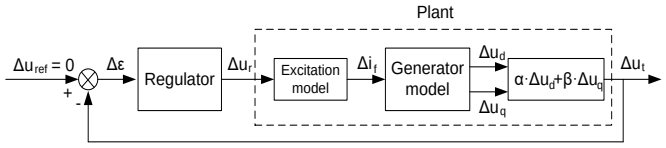

Fig. 13 Small signal control of synchronous generator

Transfer functions of the generator for d and q axis (G_{U_d}, G_{U_q}) can be derived from equation system describing the non-integer order model (14) [26]. Finally transfer function of the plant G_{plant} is given by equation (17).

$$\begin{cases} U_d = -r_s \cdot i_d - s \cdot l_{\sigma s} \cdot i_d - s \cdot l_{ad} \cdot \left(i_d - i_f + i_{1d} + i_{2d}\right) - \omega\varphi_q \\ u_f = i_f \cdot r_f + s \cdot l_{\sigma f} \cdot i_f + s \cdot l_{f12d} \cdot \left(i_f - i_{2d}\right) - s \cdot l_{ad} \cdot \left(i_d - i_f + i_{1d} + i_{2d}\right) \\ 0 = \bar{Z}_{1d}^{1/2} \cdot i_{1d} + s \cdot l_{ad} \cdot \left(i_d - i_f + i_{1d} + i_{2d}\right) \\ 0 = \bar{Z}_{2d}^{1/2} \cdot i_{2d} + s \cdot l_{ad} \cdot \left(i_d - i_f + i_{1d} + i_{2d}\right) - s \cdot l_{f12d} \cdot \left(i_f - i_{2d}\right) \\ U_q = -r_s \cdot i_q - s \cdot l_{\sigma s} \cdot i_q - s \cdot l_{aq} \cdot \left(i_q + i_{1q} + i_{2q}\right) + \omega\varphi_d \\ 0 = s \cdot l_{aq} \cdot \left(i_q + i_{1q} + i_{2q}\right) + r_{2q} \cdot i_{2q} + s \cdot l_{2q} \cdot i_{2q} \\ 0 = \bar{Z}_{1q}^{1/2} \cdot i_{1q} + s \cdot l_{aq} \cdot \left(i_q + i_{1q} + i_{2q}\right) \end{cases} \quad (14)$$

Flux components are:

$$\varphi_d = -l_{\sigma s} \cdot i_d - l_{ad} \cdot \left(i_d - i_f + i_{1d} + i_{2d}\right) \quad (15)$$

$$\varphi_q = -l_{\sigma s} \cdot i_q - l_{aq} \cdot \left(i_q + i_{1q} + i_{2q}\right) \quad (16)$$

$$G_{plant}(s) = \frac{\Delta u_t(s)}{\Delta u_r(s)} = G_{exc}(s) \cdot \left[\alpha \cdot G_{u_d}(s) + \beta \cdot G_{u_q}(s)\right] \quad (17)$$

where G_{exc} is a transfer function of an excitation system with time constant τ_e:

$$G_{exc}(s) = \frac{\Delta i_f(s)}{\Delta u_r(s)} = \frac{1}{1 + \tau_e \cdot s} \quad (18)$$

Coefficients $\alpha = 0{,}5$ and $\beta = 0{,}866$ have been chosen arbitrary for some *RL* load and operating point. Then, respectively to the variability of the parameters L_{1d}, $l_{\sigma s}$, and ω_{1d} (Table II), G_{plant} transfer function has been calculated for different magnetization levels.

According to the Fig. 14 which presents Bode diagram at variable excitation conditions of synchronous generator, one can find that the magnetic saturation has a significant influence on the frequency behaviour of the machine in the low frequency range up to 1 Hz.

Presented modelling approach is useful for synthesis of synchronous generator robust controller which has to provide proper margins for gain and phase taking into account important reparameterization of the process caused by magnetic saturation.

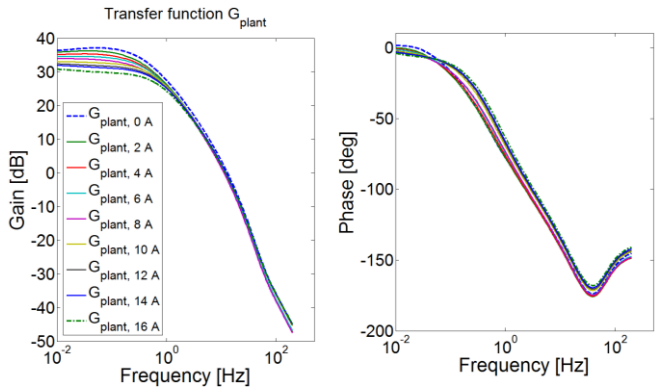

Fig. 14 Bode diagram of synchronous generator for different magnetization levels

VII. Conclusion

This paper deals with noninteger order modelling of synchronous machines which takes into account:

- diffusion of the magnetic field in massive rotor parts or damper bars of synchronous machines
- and small signal magnetic saturation.

Parameters of the noninteger *d-q* generator model have been identified with data from the SSFR test performed on the 125 kVA synchronous machine at different magnetization levels indicating significant influence on the low frequency behaviour of the machine.

It is to be noted, a coherence of the SM parameters L_{1d}, ω_{1d} change with filed current in Fig. 11, identified from the SSFR experimental measurements with the corresponding change of the parameters L_0, ω_0, obtained from the finite element analysis for a ferromagnetic sheet (Fig. 5).

Due to the fractional order, compact representation of distributed effects in the solid iron rotor core and straightforward inclusion of small signal saturation conditions this kind of modelling may be well adapted for robust control of synchronous generators in power system studies.

Appendix

Synchronous generator Elmor type GCh114o/4 rated data:
Frequency: $f_n = 50$ Hz
Voltage: $U_n = 400$ V
Power: $S_n = 125$ kVA

Per-unit values:
Frequency: $f_b = f_n = 50$ Hz
Pulsation: $\omega_b = 2*\text{pi}*f_b = 314.1593$ rad/s
Impedance: $Z_b = U_n^2 / S_n = 1.28\ \Omega$
Inductance: $L_b = Z_b / \omega_b = 0.0041$ H

References

[1] A. K. Jain, V. T. Ranganathan, "Modeling and field oriented control of salient pole wound field synchronous machine in stator flux coordinates," *IEEE Trans. on Industrial Electronics*, vol. 58 no. 3, pp. 960-970, March 2011.

[2] A. Griffo, D. Drury, T. Sawata, P.H. Mellor, "Sensorless starting of a wound-field synchronous starter/generator for aerospace applications", *IEEE Trans. on Industrial Electronics*, vol. 59 no. 9, pp. 3579-3587, Sept. 2012.

[3] M. Sautreuil, N. Retière, D. Riu, O. Sename, "A Generic Method for Robust Performance Analysis of Aircraft DC Power Systems", in *Proc. the 34th Annual Conference of the IEEE Industrial Electronics Society*, Orlando, USA, 10-13 Novembre 2008, pp. 49-54.

[4] S. Skogestad, I. Postlethwaite, *Multivariable feedback control. Analysis and design*, John Wiley & sons, 2nd edition, 2005.

[5] I. Kamwa, P. Viarouge, H. Le-Hui, J. Dickinson, "A frequency domain maximum likelihood of synchronous machine high order models using SSFR data", *IEEE Trans. on Energy Conversion*, vol. 7, pp. 525-536, Sept. 1992.

[6] I. M. Canay, "Causes of discrepancies on calculation of rotor quantities and exact equivalent diagrams of synchronous machine", *IEEE Trans. on Power Apparatus and Systems*, vol. 88, pp. 1114-1120, July 1969.

[7] I. M. Canay, "Determination of the model parameters of machines from the reactance operators", *IEEE Trans. on Energy Conversion*, vol. 8, no. 2, pp. 272-279, June 1993.

[8] A. Tessarolo, C. Bassi, D. Giulivo, "Time-stepping finite-element analysis of a 14-MVA salient pole shipboard alternator for different damper winding design solutions," *IEEE Trans. on Industrial Electronics*, vol. 59 no. 6, pp. 2524-2535, June. 2012.

[9] D. Riu, N. Retière, M. Ivanes, "Induced currents modeling by half-order systems application to hydro- and turbo-alternators", *IEEE Trans. on Energy Conversion*, vol. 18, pp. 94-99, March 2003.

[10] S. Racewicz, D. Riu, N. Retière, P. J. Chrzan, "Non linear half-order modelling of synchronous machine", in *IEMDC 2009*, Miami, Florida, May 2009, p. 778-783.

[11] *IEEE Guide for synchronous generator modeling practices in stability analyses*, IEEE Standards Board 1991.

[12] S.H. Minnich, "Small signals, large signals and saturation in generator modelling", *IEEE Trans. on Energy Conversion*, vol. EC-1, no. 1, pp. 94-102, March 1986.

[13] D. C. Aliprantes, S. D. Sudhoff, B. T. Kuhn, „A synchronous machine model with saturation and arbitrary rotor network representation", *IEEE Trans. on Energy Conversion*, vol. 20, pp. 584-594, Sept 2005.
[14] M. L. Awad, G. R. Slemon, M. R. Iravani, "Distributed steady state nonlinear modelling of turboalternators", *IEEE Trans. on Energy Conversion*, vol. 15, no. 3, pp. 233-239, 2000.
[15] Xiaodong Liang, A. M. El-Serafi, S. O. Faried, "Application of the Finite-Element Method for the Determination of the Parameters Representing the Cross-Magnetizing in Saturated Synchronous Machines", *IEEE Trans. on Energy Conversion*, vol. 25, pp. 70-79, 2010.
[16] E. Levi, V. A. Levi, "Impact of dynamic cross-saturation of saturated synchronous machine models" *IEEE Trans. on Energy Conversion*, vol. 15, no. 2, pp. 224-230, 2000
[17] P. L. Alger, *Induction Machines*, NewYork: Gordon and Breach, 1970.
[18] S. Racewicz, D. Riu, N. Retière, P. J. Chrzan, "Half-order modelling of turboalternators – An adapted method of parameter identification", in *ICEM 2006*, Chania, Crete Island, September 2006, CD-ROM Session PSA2-5, ref. 127, pp. 1-6.
[19] S. Racewicz, D. M. Riu, N. M. Retière, G. Meunier, P. Labie, P. J. Chrzan, "Half-order modelling of ferromagnetic sheet. Validation with finite elements simulation", in *EPNC 2008*, Lille, France, July 2008, pp. 11-12.
[20] S. Racewicz, D. M. Riu, N. M. Retière, P. J. Chrzan, "Half-order modelling of ferromagnetic sheet", in *ISIE 2011*, Gdansk, Poland, 27-30 June 2011.
[21] *IEEE Guide for Test Procedures for Synchronous Machines*, IEEE Std 115, 2009.
[22] J. Verbeeck, R. Pintelon, P. Lataire, "Influence of saturation on estimated synchronous machine parameters in standstill frequency response tests", *IEEE Trans. on Energy Conversion*, vol. 15, no. 3, pp. 277-283, 2000.
[23] F. S. Sellschopp, M. A. Arjona, „Determination of Synchronous Machine Parameters Using Standstill Frequency Response Tests at Different Excitation Levels", *IEEE Int. Electric Machines & Drives Conference IEMDC'07*, vol. 2, pp. 1014-1019, May 2007.
[24] Gh. Ahrabian, A. M. El-Serafi, "Identification of the synchronous machine parameters under magnetic saturated conditions using Stand Still Frequency Response Test", presented at Canadian Conference on Electrical and Computer Engineering, 2001.
[25] J. F. Gieras, M. Wing, Permanent magnet motor technology, Marcel Dekker, Inc. 1997.
[26] S. Racewicz, P. J. Chrzan, D. M. Riu, N. M. Retière, "Time domain simulations of synchronous generator modelled by half-order system", in *IECON 2012*, Montreal, Canada, 25-28 October 2012.